Report for Current Biology (2500 words of main text and may have up to 4 display items [Figures + Tables])

Evolutionarily diverse fungal zoospores show contrasting swimming patterns specific to ultrastructure.

Luis Javier Galindo[1, *], Thomas A. Richards[1], Jasmine A. Nirody[2, *]

[1] Department of Biology, University of Oxford, Oxford, United Kingdom
[2] Department of Organismal Biology and Anatomy, University of Chicago, Chicago, IL, USA

Author for correspondence:
Jasmine A. Nirody (lead contact) or Luis Javier Galindo
*e-mail: jnirody@uchicago.edu; luisjagg92@gmail.com

Keywords: motility, zoospores, tubulin, ultrastructure, chytrid, fungi, light-sensing, phototaxis

Summary (250 words)

Zoosporic fungi, also called chytrids, produce single celled motile spores with flagellar swimming tails (zoospores)[1,2]. These fungi are key components of aquatic food webs, acting as pathogens, saprotrophs and prey[3–8]. Little is known about the swimming behaviour of fungal zoospores, a crucial factor governing dispersal, biogeographical range, ecological function and infection dynamics[6,9]. Here, we track the swimming patterns of zoospores from 12 evolutionary divergent species of zoosporic fungi from across seven orders of the Chytridiomycota and the Blastocladiomycota. We report two major swimming patterns which correlate with the cytoskeletal ultrastructure of these zoospores. Specifically, we show that species without major cytoplasmic tubulin components swim in a circular fashion, while species with prominent cytoplasmic tubulin structures swim in a pattern akin to a random walk (move-stop-redirect-move). We confirm cytoskeleton architecture by performing fluorescence confocal microscopy across all 12 species. We then treat representative species with variant swimming behaviours and cytoplasmic-cytoskeletal arrangements with tubulin stabilizing (Taxol) and depolymerizing (Nocodazole) pharmacological compounds. We observed that when treating the 'random walk' species with Nocodazole their swimming behaviour changes to a circular swimming pattern. Confocal imaging of the nocodazole-treated zoospores demonstrates these cells maintain flagellum tubulin structures but lack their characteristic cytoplasmic tubulin structures. Our data demonstrate that the capability of zoospores to

perform 'complex' random walk movement is linked to the presence of prominent cytoplasmic tubulin structures and suggests a link between cytology, sensory systems, and swimming behaviour in a diversity of zoosporic fungi.

Results and discussion

Differential swimming in variant chytrids

Most chytrid species form uniflagellated zoospores, with only a few species developing multiflagellated zoospores (e.g., *Neocallimastix* and *Piromyces*[10]) or spores without flagella (e.g., *Hyaloraphidium*[11]). Zoospores can move using two distinct cellular mechanisms: swimming propelled by beating of the tubulin articulated flagellum[3,12]; or amoeboid crawling using actin driven pseudopodia[13,14]. Crawling is an adaptation for traveling short distances on surfaces (e.g., exploration of trophic substrate[15]). In contrast, flagellum-based swimming is ideal for medium range dispersal across aquatic environments[9]. Thus, swimming plays an important role in facilitating the trophic life cycle of these fungi, a function that is often governed by chemo- or photo-taxis[16–19].

To explore swimming function in chytrid fungi we analysed the patterns of movement for zoospores from 12 species from the two major phyla: Chytridiomycota and Blastocladiomycota. These include eight Chytridiomycota species grouped into six orders: *Synchytrium microbalum* (Synchytriales), *Clydaea vesicula* (Lobulomycetales), *Chytriomyces hyalinus* (Chytridiales), *Rhizoclosmatium globosum* (Chytridiales), *Homolaphlyctis polyrhiza* (Rhizophydiales), *Rhizophlyctis rosea* (Rhizophlyctidiales), *Geranomyces variabilis* (Spizellomycetales), and *Spizellomyces punctatus* (Spizellomycetales); and four species of Blastocladiomycota from the order Blastocladiales: *Catenophlyctis* sp. (Catenariaceae), *Blastocladiella emersonii*, *Allomyces macrogynus* and *Allomyces reticulatus* (Blastocladiaceae).

We find that medium-range motility patterns (swimming trajectories measured over tens of seconds) varied markedly among different species (Figure 1), with the zoospores from four species of Chytridiomycota (*S. microbalum*, *C. hyalinus*, *R. globosum* and *H. polyrhiza*) swimming in a circular pattern. In contrast, all zoospores from species of Blastocladiomycota tested and four different species of Chytridiomycota (*C. vesicula*, *R. rosea*, *G. variabilis* and *S. punctatus*) swim using a pattern akin to a random walk (move-stop-redirect-move; Figure 1A). To investigate this pattern further, we plotted the distribution of reorientation (turn) angles and the mean square displacement (MSD) of these 12 movement patterns to characterize motility dynamics at both shorter and longer timescales, respectively (see the methods for the mathematical formulae). Such methods can be used to quantitatively differentiate random walk and circular motility patterns[20,21]. Circular swimming cells are expected to reorient themselves more consistently than those swimming in a random walk pattern, resulting in a narrower

distribution of turn angles. For cells exhibiting circular motility patterns, the MSD plot should form a plateau in the later phases of the MSDs plots. Consistent with the conclusions from our primary observations (Figure 1A), we find that reorientation angle distributions are indeed generally narrower for circular swimming zoospores (Figure 1B), and that the MSD plateaus at shorter timescales for these species in comparison to the other zoosporic fungi species which swim in random walk patterns (Figure 1C). We note that the random walk swimmer *A. macrogynus* (*Am*) shows a narrower distribution and the circular swimmer *C. hyalinus* (*Ch*) shows a broader angle range when compared to chytrids with similar swimming behaviours. This is because *Am* tends to swim in more regular, directed trajectories than other random walkers; this is also apparent from the MSD plot which scales with a higher exponent than that of other species (this inconsistency is discussed further below). On the other hand, *Ch* is the circular-swimmer with the most variable radii, resulting in a wider turn angle distribution. We expect that differences in species-specific behaviours will be further heightened in experiments conducted with greater imaging resolution (e.g., using a camera with a higher frame rate). Apart from slightly higher speeds observed in *H. polyrhiza*, no significant differences in instantaneous swimming speed were observed across the 12 species (Figure S3A), suggesting the difference in movement behaviour is a product of cellular mechanics and not propulsion velocity.

Our results provide support for a primary conclusion that zoosporic fungi show two distinct swimming patterns, circular and a random walk. These patterns have previously been noted in a subset of chytrid fungi. Specifically, circular swimming in the zoospores of the Rhizophydiales chytrid *Rhizophydium planktonicum*[22] and random walk swimming patterns in the zoospores of the Blastocladiomycota *Paraphysoderma sedebokerense*[14] and *Physoderma* spp.[23] from the order Physodermatales. These additional observations support our results and suggest that a wider diversity of chytrid zoospore swim using two fundamentally different general patterns.

An association between zoospore swimming pattern and cytoplasmic tubulin structures

To gain insights into the cellular mechanisms which putatively underpin these differences in swimming patterns, we performed fluorescent confocal microscopy of the 12 species studied using antibodies and cytological stains against α-tubulin, actin and the lipid components of the zoospores (Figure 2). To further support our observations we reviewed previous electron microscope studies[24–31] (Table S1). These results suggest that observed variation in motility

patterns segregate with cytological characters, specifically the presence of prominent cytoplasmic tubulin structures, and not by higher taxonomic classification (Figures 1, 2, 3A).

In all four Blastocladiomycota species, we show that the cytoplasmic tubulin microtubules create prominent and complex cytoskeletal arrays or 'ribs' within the cell body which extend from the kinetosome of the flagellum around the periphery of the main body of the cell (n ≥ 10 - Figures 3B1, E1, H1 and K1). Our microscopy shows that an actin cytoskeleton is less apparent (Figure 2, 3A; n ≥ 10 cells observed for each species). Similarly, for two Chytridiomycota species that show random walk movement patterns, *S. punctatus* and *G. variabilis* (Spizellomycetales) we also observe prominent tubulin microtubules that radiate into the zoospore cytoplasm from the kinetosome (n ≥ 10 - Figures 3Z1, C2). These microtubules have been observed in previous ultrastructural TEM-based studies[25,28,31,32] (Table S1). For these Spizellomycetales, actin is present and forms patches in both species (the presence of these patches indicates possible actin organisation centres[15,33]).

Two additional random walk Chytridiomycota species also showed prominent cytoplasmic α-tubulin-stained material; *R. rosea* and *C. vesicula*. Although these were not organised as clearly defined ribs in our micrograph analyses, such cell forms also performed random walk movement behaviours. The zoospores of *R. rosea* (n = 10) showed both seemingly randomly arrayed α-tubulin accumulations and actin patches through-out the cytoplasm. Interestingly, microscopy imaging of *C. vesicula* identified an additional distinct α-tubulin organisation consisting of a peripheral cytoplasmic mesh of microtubule structures (n = 10 - Figure 3Q1). These α-tubulin-stained structures were not detected in the original TEM-based descriptions for both sepcies[27,30]. However, the strains of *R. rosea* (JEL0764) and *C. vesicula* (JEL0476) used, are different to the strains investigated in the original descriptions (Barr186/BR186 and JEL369 respectively[27,30,34]) so some variation in cytoskeletal structure may be present within these species complexes. Additionally, these observations were made using TEM[27,30], thus, these analyses would fail to detect non-electron dense dissociated tubulin material like the cytoplasmic structures detected for *R. rosea* and *C. vesicula* in our analyses (Figure 2Q1, W1). In *C. vesicula* we observe cytoplasmic actin co-localizing with the canonical vesicles found near the kinetosome of this species[27] (Figure 2). *R. rosea* zoospores also have a large fibrillar rhizoplast extending from kinetosome which may be involved in controlling movement[30] (Table S1).

In contrast to the previously described Chytridiomycota species, we find no prominent tubulin structures in the cytoplasm of the circular-swimming zoospores of *S. microbalum* (Synchytriales), *H. polyrhiza* (Rhizophydiales), *C. hyalinus*, and *R. globosum* (Chytridiales) (n ≥ 10 cells observed for each species - Figure 2, 3A, Table S1). Furthermore, in these four Chytridiomycota actin is the only cytoplasmic-cytoskeletal protein detected. It is important to note that we refer to these cytoplasmic tubulin structures as 'prominent' because we are aware

that in the zoospores of *C. hyalinus*, *R. globosum* and *H. polyrhiza* there are minor cytoplasmic tubulin components in the form of small bundles of microtubules connecting the kinetosome with the lipid-organelle and its associated rumposome (Figure 3A). These tubulin structures have been observed using TEM[35] (Table S1).

To our knowledge, this is the first systematic study of swimming patterns across a wide representation of the chytrids with the patterns identified placed into a cellular and phylogenetic context (Figure 3A). Our analyses confirm that the presence of prominent cytoplasmic tubulin of various arrangements correlates with different swimming patterns. Specifically, zoospores from Chytridiomycota species that lack prominent cytoplasmic tubulin structures swim in a circular pattern. In contrast, all four Blastocladiomycota species and those Chytridiomycota species which have prominent α-tubulin-stained structures within their cytoplasm, manifest a random walk swimming pattern (Figure 3A).

Lastly, by performing live-fluorescent imaging of *B. emersonii* (*Be*) zoospores after staining with Nile Red lipid stain (n = 50) we identified that the random walk pattern is characterized by straight movements, followed by a stop and redirection of the cellular body towards the side in which the lipid body is located. These observation in *Be* led to the hypothesis that re-direction in random walk movement occurs by hinge-like bending at the area between the cytoplasmic microtubular structures and the flagellar kinetosome, and in an angle greater than the final angle of movement (Figure 3B). Alternatively, cells without prominent tubulin cytoplasmic structures lack this hinge-like articulation, thus, are restricted to swim using circular/spiral patterns.

Pharmacological inhibition demonstrates tubulin structures determine how random walker cells reorient

To test the involvement of tubulin cytoplasmic structures in their swimming patterns, we treated representative species of each swimming behaviour and cytoplasmic cytoskeletal type with 1 μM of tubulin stabilizing (Taxol) or depolymerizing (Nocodazole) drugs. These drugs have successfully been used on several microbial eukaryotes to study cytoplasmic and flagellar tubulin-based structures[36–40]. We selected *B. emersonii* (*Be*; Blastocladiomycota) and *S. punctatus* (*Sp*; Chytridiomycota) given their prominent microtubular ribs and marked random walk movement, and *R. globosum* (*Rg*; Chytridiomycota) due to its lack of major tubulin cytoplasmic structures, circular swimming and the increasing utility of this species as a model system[41].

We observed that when treating random walk species *Be* and *Sp* with nocodazole their swimming behaviour changes to manifest a circular swimming pattern, as shown by their MSD plots reaching plateau (Figure 4A). However, there was no observable change in the swimming behaviour of the circular swimming *Rg* zoospores treated with nocodazole. All taxol-

treated zoospores showed no change in their swimming patterns. After imaging these nocodazole-treated and taxol-treated zoospores, we confirmed that nocodazole-treated zoospores lack their characteristic tubulin rib-like cytoplasmic arrangements, while there was no change in the tubulin arrangement of the taxol-treated species (Figure 4B-G). We also note that for the nocodazole-treated *Be* zoospores the lipid component, which is usually located to one side next to the base of the flagellum, loses its posterior cellular position and is relocated randomly within the cell possibly towards the anterior side (Figure 4C2).

We note neither drug stopped flagellum swimming and in all three test species tubulin structures of the flagellum showed no major structural changes besides a putative and minor reduction in flagellar length in nocodazole-treated *Be* (Figure 4). Flagellar length does not seem to be factor determining the observed swimming patterns. All described zoospores vary in their flagellar length regardless of their swimming patterns, and species with the same flagellar length (e.g., ~20 µm) can present either circular (e.g., *C. hyalinus*) or random walk movement patterns (e.g., *S. punctatus*) (Table S1). In our test species *Rg* retains a long flagella and circular swimming across all treatments and after nocodazole treatment *Sp* retains a similar flagellar length, but the movement behaviour is transformed to a circular swimming mode.

Our results demonstrate that we succeeded in inhibiting the polymerization/formation of ribs within the main body of *Be* and *Sp* zoospores which became circular swimmers after treatment (Figure 4). Thus, we conclude that the capability of zoospores to perform 'complex' movements in a random walk fashion is linked to the presence of prominent cytoplasmic tubulin structures. Overall, these findings demonstrate that a prominent tubulin-cytoplasmic component may allow zoospores to swim using intricate patterns in which they can redirect movement by using a hinge-like articulation, the random walk pattern.

We performed an additional series of controls to test the involvement of actin in zoospore swimming behaviour by using actin depolymerizing drugs (Cytochalasin D, Latrunculin B and Jasplakinolide). As observed previously for *Batrachochytrium dendrobatidis*[43] these drugs caused mass zoospore encystation in all three species, and no change in the swimming behaviour of the few remaining swimming zoospores was observed (Figure S4).

Is movement pattern connected to light-sensing and to the lipid organelle in these zoospores?

Regarding the lipid component of chytrid zoospores, in Chytridiomycota we consistently observed one large lipid globule in all species ($n \geq 10$), with one exception found in *R. rosea* in which we identified numerous small lipid droplets, a characteristic of this Chytridiomycota species[30] (Figure 2). In Blastocladiomycota species we consistently observed clusters of

several lipid globules (n ≥ 10 – for these four species), usually located towards the flagellum (Figure 2).

The arrangement of these lipid organelles is diverse (Figure 2, 3A) and are referred to as the microbody-lipid globule complex (MLCs)[35]. MLCs are structures thought to be involved in storage and production of chemical energy for flagellar beating[35] although other functions are possible. These structures are composed of microbodies, mitochondria, ribosomes and one or more large membrane-enclosed lipid globule (Figure 2, 3A)[2,35]. Using Powell's (1978) classification[35] all MLCs discussed here from Chytridiomycota are classified as type 1, which can be classified as A or B; depending on the respective absence or presence of a rumposome (a cisterna-like disc of membranous tubules); zoospores can be further classified as A/B_1 or A/B_2 depending on the arrangement of different cellular components. On the other hand, the lipid-filled MLC organelles from Blastocladiomycota are type 4, and can alternatively be referred to as side-body complexes (SBCs) (Figure 2, 3A)[1,25,35,44].

In addition to energetics, these organelles have been hypothesised to be involved in light perception[17,42,45,46]. Indeed, *Blastocladiella emersonii* and *Allomyces reticulatus* zoospores show positive phototaxis[17,18,47,48]. In particular, the SBC of *B. emersonii* was found to be in close spatial association with a layer of RGC (or CyclOp) proteins (a fusion protein composed of a type I microbial rhodopsin and guanylyl cyclase enzyme domain) which participates in a cGMP-mediated light-sensing pathway[17,49,50] by controlling flagellar activation from its localization next to the SBC. Both these systems are in close physical association at the base of the flagellum. Recent analyses suggest that the molecular elements necessary for a functional RGC based light sensing pathway are present in the eight of the twelve fungal species analysed here[45,51,52]. These include six species with homodimeric RGC variants (all four Blastocladiomycota species, *S. microbalum* and *H. polyrhiza*) and two species with heterodimeric RGC complexes (Chytridiales: *C. hyalinus*, *R. globosum*) (Figure 3A), which consist of two subunits with distinct photochemical properties which evolved from an ancient duplication of the RGC gene[51,52]. We observe no association between RGC type, swimming pattern and ultrastructure. However, within the Chytridiomycota analysed here, those species which swim in circular patterns possess RGCs genes and MLCs type 1B and those with random walk movement lack RGCs and have MLCs type 1A (Figure 3A), but wider sampling is needed to test this pattern.

However, some swimming behaviours clearly seem to be influenced by the presence of the MLC. Particularly, *Be* produces zoospores with the RGC system and that swim in a random walk pattern and its SBC is found at one side of the kinetosome. Our live-imaging experiments show that the cell-bending and redirection of motion in *Be* zoospores occurs towards the side of the cell in which the SBC is present (Figure 3B). Among the possible explanations could be that the prominent SBC is structurally restraining the movement of the

Be zoospores towards that side, or that the zoospore moves towards the direction in which the light sensing organelle gets its stimulus. The position of MLCs relative to their movement is harder to assess in Chytridiomycota species, given their small cellular sizes and MLCs, which are generally more loosely located within the cell. Lastly, fluorescent confocal microscopy revealed that nocodazole-treated *Be* zoospores not only lacked cytoplasmic tubulin microtubules, but they also lost the typical arrangement of the SBC organelle at the base of the flagellum, providing further evidence that its positioning is dependent on tubulin structures (Figure 4C). The physical link between the SBC and the base of the kinetosome may therefore be essential for the transduction of the light signal to flagellar movement which then translates to the observed swimming pattern.

Lastly, we show that *A. macrogynus* (*Am*) tends to swim in more regular, directed trajectories than other random walkers; as shown by its a narrower angle range distribution and a high MSD exponent (Figure 1B-C). One possible explanation is that *Am* is the only Blastocladiomycota in our sample known to have replaced light-sensing with chemo-sensing[18]. If our set up is triggering constant re-orientation by light sensing (all observations are under undirected white light stimulus) but not by chemo sensing (no amino acid gradients), it would explain the broad angle distribution observed in all Blastocladiomycota except in *Am*, which has no response to light. Overall, these experiments point towards a link between zoospore ultrastructure, movement, and the light sensing organelle component. Our findings provide comparative model systems for further exploration of the link between cytology, sensing and divergent motility behaviour in single-celled eukaryotic microbes.

Acknowledgements

We gratefully acknowledge the Micron Advanced Bioimaging Facility (supported by Wellcome Strategic Awards 091911/B/10/Z and 107457/Z/15/Z). We also acknowledge Suely Lopes Gomes (Universidade de São Paulo) for inspiring work on chytrid light perception. This work was funded by the Horizon 2020 research and innovation programme under the European Marie Skłodowska-Curie Individual Fellowship H2020-MSCA-IF-2020 (grant agreement no. 101022101—FungEye) and Leverhulme Trust Project Grant (RPG-2022-234; The evolutionary diversification of a sub-cellular fungal eye). T.A.R. is supported by a Royal Society URF (URF/R/191005). J.A.N. acknowledges support from All Souls College, Oxford, from the National Science Foundation through the Center for Living Systems at the University of Chicago (grant no. 2317138), and from the NSF-Simons National Institute for Theory and Mathematics in Biology, which is jointly supported by the U.S. National Science Foundation (award 2235451) and the Simons Foundation (award MP-TMPS-00005320). We are also

grateful for the comments of three anonymous reviewers, which have improved this manuscript.

Author contributions

L.J.G., T.A.R. and J.N.: conceived the study; L.J.G.: microscopy imaging, drug assays and manuscript writing; T.A.R. manuscript writing; J.N.: image and mathematical analyses and manuscript writing. All authors gave final approval for publication and agreed to be held accountable for the work performed therein.

Declaration of Interests

These authors declare no competing interests.

Figure 1. Movement tracks for 12 zoosporic fungal species. (A) Tracks show cytology-specific swimming pattern behaviours, with all Blastocladiomycota species and Chytridiomycota species possessing prominent tubulin-based cytoplasmic structures swimming in a random walk pattern, while Chytridiomycota zoospores without prominent cytoplasmic tubulin structures swim in circular movements. Composite tracks are shown compiled into a single plot with starting points (time = 0) centred at the point of origin. (B) Distribution of turn (reorientation) angles for each group of zoospores (Blastocladiomycota species, Chytridiomycota species with prominent tubulin-based cytoplasmic components, and Chytridiomycota species with no prominent tubulin-based cytoplasmic structures). Species-averaged distributions are shown as partially transparent lines, as labelled. (C) Ensemble- and time-averaged mean-squared displacement (MSD) for each group of zoospores. Species-averaged MSDs are shown as partially transparent lines, as labelled. For effective comparison between groups, MSD plots are normalised by the initial value (at time lag 1) for each species. Unnormalized MSDs for each cell are shown in Figure S3B. Labels: *Catenophlyctis sp.: Cat, Blastocladiella emersonii: Be, Allomyces macrogynus: Am, Allomyces reticulatus: Ar, Synchytrium microbalum: Sm, Clydaea vesicula: Cv, Chytriomyces hyalinus: Ch, Rhizoclosmatium globosum: Rg, Homolaphlyctis polyrhiza: Hp, Rhizophlyctis rosea: Rr, Geranomyces variabilis: Gv,* and *Spizellomyces punctatus: Sp.*

Figure 2. Ultrastructure of Blastocladiomycota and Chytridiomycota zoospores. First columns show brightfield phase contrast confocal microscopy images; second columns show fluorescent confocal microscopy micrograph of the zoospore; third columns show the merged images of brightfield and fluorescent channels. Microscopy images were taken and stained using the methods described in Galindo et al. (2022)[45] with Nile Red to stain lipid droplets, α-tubulin DM1A + Alexa Fluor 647 to stain tubulin and Alexa Fluor 488 Phalloidin to stain actin. In micrographs α-tubulin structures are stained magenta, actin stained cyan, and the lipid

bodies (proposed to function as a light-sensing organelle) are stained yellow (see Figures S1-2 for individual fluorescent channels). In the fluorescent channel panels for those species which possess cytoplasmic α-tubulin staining there is a small panel detailing the α-tubulin component. Species/micrographs bracketed/highlighted with red - belong to the Blastocladiomycota and those species micrographs with green-to-pink highlight-brackets correspond to Chytridiomycota from the: Synchytriales (M1-O1), Lobulomycetales (P1-L1), Chytridiales (M1-R1), Rhizophydiales (S1-U1), Rhizophlyctidiales (V1-X1) and Spizellomycetales (Y1-D2), respectively (the same colour code is used in Figure 3). Scale bars: A1-O1 = 10 μm; P1-D2 = 5 μm. Scale bars in small α-tubulin panels: B1, E1, H1 = 10 μm; K1, Q1, W1, Z1 and C2 = 5 μm. Labels: *Catenophlyctis sp.: Cat, Blastocladiella emersonii: Be, Allomyces macrogynus: Am, Allomyces reticulatus: Ar, Synchytrium microbalum: Sm, Clydaea vesicula: Cv, Chytriomyces hyalinus: Ch, Rhizoclosmatium globosum: Rg, Homolaphlyctis polyrhiza: Hp, Rhizophlyctis rosea: Rr, Geranomyces variabilis: Gv,* and *Spizellomyces punctatus: Sp.*

Figure 3. Depiction of motility, ultrastructure and phylogenetic relationships of the zoosporic fungal species from this study. (A) Phylogenetic tree is adapted from Amses et al. 2022[53] showing the absence (black branches) or presence of homodimeric (yellow branches) or heterodimeric (magenta branches) RGCs opsin complexes (adapted from Broser et al. 2023[52]). Illustrations depict the overall ultrastructure of each zoospore including their lipid (yellow), actin (cyan), and α-tubulin-based components (magenta). A representative trajectory highlighting the overall movement pattern of each species is shown to the right of each drawing and grouped by a continuous (circular pattern) or discontinuous line (random walk pattern). Number in parentheses bellow the species names and main branches indicate the lipid-organelle MLC type of each zoospore according to Powell's (1978) classification[35]. See Table S1 for references. (B) Random walk swimming pattern hypothesis based on our findings in *B. emersonii* zoospores.

Figure 4. Movement tracks and confocal imaging of fungal zoospore from three chytrid species after treatment with Nocodazole and Taxol. (A) Representative swimming patterns and ensemble- and time-averaged mean-squared displacement (MSD) for each treatment in three zoospores fungal species (see Figure S4 for further treatments). (B1-G5) Confocal imaging of drug treated zoospores. The first column shows brightfield phase contrast confocal microscopy images (B1-G1); second column shows in yellow the channel for Nile Red staining of lipid droplets (B2-G2); third column shows in magenta α-tubulin DM1A + Alexa Fluor 647 staining of α-tubulin (B3-G3); fourth column shows the fluorescent channel merged (B4-G4); fifth column shows the merged images of brightfield and fluorescent channels (B5-G5). Scale

bars = 10 µm. *Blastocladiella emersonii: Be, Spizellomyces punctatus: Sp, Rhizoclosmatium globosum: Rg.*

STAR Methods

Resource availability

Lead contact

Further information and requests for resources and reagents should be directed to and will be fulfilled by the Lead Contact, Jasmine A. Nirody (jnirody@uchicago.edu).

Materials availability

This study did not generate any new or unique reagents.

Data and code availability

All data are available in the figures, tables, and data files associated with this manuscript. Plots of all tracks for each species are shown in Supplementary Material. Raw videos are available at https://figshare.com/account/home#/projects/207943 and tracking data, detailed protocols, and analysis codes are provided at http://github.com/jnirody/fungalzoospores. Raw confocal microscopic images can be found at: https://figshare.com/projects/FungEye/132734. Any additional information required to reanalyse the data reported in this work paper is available from the Lead Contact upon request.

Experimental model and subject details

Cultures of *Blastocladiella emersonii* ATCC 22665 (ATCC; American Type Culture Collection), *Catenophlyctis* sp. JEL0575 (CZEUM; Collection of Zoosporic Eufungi at University of Michigan; 18S rDNA sequence could indicate it belongs to a species of *Catenaria*[34]), *Clydaea vesicula* JEL0476 (CZEUM), *Chytriomyces hyalinus* CBS 675.73 (previously referred as *C. confervae* given that CBS 675.73 = ATCC 24931 = Barr 97 and Barr 97 is *C. hyalinus* [34,54]; Westerdijk Fungal Biodiversity Institute), *Homolaphlyctis polyrhiza* JEL0142 (CZEUM), *Rhizophlyctis rosea* JEL0764 (CZEUM), *Geranomyces variabilis* JEL0559 (CZEUM), and *Spizellomyces punctatus* SW1 (CZEUM) were vegetatively grown in 25 cm2 culture flasks (Sarstedt) filled with 25 mL of PYG liquid media (0.13% w/v peptone, 0.13% w/v yeast extract, 0.3% w/v glucose). *Rhizoclosmatium globosum* JEL0800 (CZEUM) vegetative cells were grown on PYG agar plates (0.13% w/v peptone, 0.13% w/v yeast extract, 0.3% w/v glucose, and 1.5% w/v agar). *Allomyces macrogynus* Australia_3 (CZEUM) and *Allomyces reticulatus* ATCC 42465 (ATCC) was grown in 25 cm^2 culture flasks filled with 25 mL of Emerson YpSs/4 liquid media (0.1% w/v yeast extract, 0.375% w/v soluble starch, 0.025% w/v dipotassium

phosphate, 0.01% w/v magnesium sulfate). *Synchytrium microbalum* JEL0517 (CZEUM) vegetative cells were grown on PYG agar plates (0.13% w/v peptone, 0.13% w/v yeast extract, 0.3% w/v glucose, and 1.5% w/v agar) and in PYG liquid media (0.13% w/v peptone, 0.13% w/v yeast extract, 0.3% w/v glucose). All fungal vegetative growth was performed at 21°C and transferred every two weeks by inoculating 25 µl of previous culture to a new flask/plate containing 25 ml of media.

To induce sporulation of *B. emersonii* ATCC 22665, *C. vesicula* JEL0476, *C. hyalinus* CBS 675.73, *H. polyrhiza* JEL0142, *R. rosea* JEL0764, *G. variabilis* JEL0559, and *S. punctatus* SW1, 200 mL of liquid PYG were inoculated with 20 ml of vegetative cells in 175 cm^2 culture flasks (Sarstedt), and incubated, with 150 rpm agitation, for 24 h at 21°C. To induce sporulation in *A. macrogynus* Australia_3, *A. reticulatus* ATCC 42465 and *Catenophlyctis* sp. JEL0575 vegetative growth was performed for ~5 days in 25 ml of liquid YpSs/4 (*Allomyces*) or PYG (*Catenophlyctis*). Sporangia were then separated from the culture using sterile tweezers, washed with distilled H_2O, and placed in 20 mL of distilled H_2O in a 25cm^2 culture flask at 21°C overnight. *R. globosum* JEL0800 and *S. microbalum* JEL0517 zoospore obtention was performed by growing this strain on PYG agar plates for 4 days. Plates were then flooded with 7 mL of distilled H_2O and after resting for 15 min to allow sporulation, zoospore-containing H_2O was transferred to a 15 ml falcon tube. Zoospores were then separated from sporangia using a 20 µm pluriStrainer (pluriSelect) into 50 ml falcon tubes. All sporulation inductions were performed at 21°C.

Method details

Images acquisition

Out of the 12 obtained liquid zoospore solutions, seven were PYG-based and five were H_2O -based (*A. macrogynus*, *A. reticulatus*, *Catenophlyctis* sp., *S. microbalum* and *R. globosum*). After sporulation, both 7 µl and 100 µl of zoospore suspension aliquots were placed respectively on a slide and coverslip or placed on the bottom of the well of a flat bottom 86-well plate. *S. microbalum* was recorded only on plates and *A. reticulatus* culture died before plate videos could be recorded. Thus, we image zoospores both in a physically constrained and non-constrained environment; we observed no difference between the two conditions (Figure S3C). Alternatively, Nile Red (Thermo Fisher Scientific, Cat# N1142) was added in a 1:500 v/v concentration for 5 min before live-imaging of zoospores. Cells were imaged on an Olympus CKX53 inverted microscope with 10X, 20X, and 40X objectives according to the size of the zoospores and/or their swimming trajectories. Videos of 15 to 30 seconds were taken at 60 fps with a Std Chromyx HD camera mounted on a U-TV0.5XC-3-8 0.5x C-Mount Adapter.

Exposures, focus, and stage position were kept constant while recording for motility analyses. The number of trials *n* recorded for each species is shown in Figure 1A.

Both PYG media and H_2O have similar physical conditions and the use of different liquid media did not seem to affect the swimming behaviours of closely related species with similar cellular structures (e.g., circular swimming: *R. globosum* in H_2O and *C. hyalinus* in PYG medium; random walk swimming: *A. reticulatus* in H_2O and *B. emersonii* in PYG medium). We note that given the small size of the zoospores, minor changes in media viscosity are unlikely to affect cell mechanics. However, it is possible that environmental chemistry and the presence of different ion concentrations in the aqueous environment may modify swimming behaviour[55,56]. To explore this source of variation further, we re-recorded the swimming behaviour of zoospores of the 7 species which were originally recorded in PYG media also in distilled H_2O media (by filtering and re-suspension in dH_2O). We observed no change in the swimming patterns when moved to alternative media (Figure S3D).

Tracking and motility analysis

Movies of swimming zoospores were viewed in FIJI[57], and movement was tracked using a semi-automated protocol with the TrackMate plugin[58]. Before tracking, videos were pre-processed as follows: (1) the background was subtracted; (2) artifacts were detected and removed by subtracting the median image of the video from each frame. Cells were segmented using TrackMate's Difference of Gaussian detector; manual quality control by eye was performed on the first frame for each video. The centre-of-mass of segmented images were joined to create tracks using a Linear Assignment Problem (LAP) tracker; maximum gap closing was set at 50 pixels and maximum frame gap at 10 frames. Final quality control of all tracks was performed using TrackScheme to ensure each track consisted of only one detected spot per frame.

Drug assays

Drugs assays were conducted by exposing cultures of *B. emersonii*, *S. punctatus* (grown overnight) and *R. globosum* (grown for 4-days) for 5 hours at 21°C to 1 µM of Nocodazole (tubulin polymerization inhibition) and separately Taxol (microtubule stabilizing) solution resuspended in DMSO. Zoospores were strained-filtered from sporangia as described before and then fixed in 4% *w/v* paraformaldehyde (for confocal imaging) and/or video recording. Aliquots of zoospore solution of these three species were also exposed for 10 min at room temperature to 1 µM Latrunculin B (a drug which sequesters actin monomers), 100 µM Cytochalasin D (a drug which caps actin filaments), 10 µM Jasplakinolide (a drug which stabilizes actin filaments) solutions and then resuspended on DMSO for movement behaviour video recording. Protocols and drug concentrations were based on previous studies using

these same drug treatments on either zoosporic fungi and/or alternative microbial eukaryotes[36–40,43,59].

Quantification and statistical analysis

Plotting of tracks and quantitative motility metrics were performed from exported COM data using in-house scripts written in Python. Random walk and circular motility patterns were quantitatively differentiated using reorientation angle (or turn angle), a measure of local cellular behaviour, and mean square displacement (MSD), a measure of the deviation of the position of a cell *r* over time. Turn angles at time *t* were calculated as: $\delta\Theta = \tan -1\,[\mathbf{v}(t) \times \mathbf{v}(t+1))\,/\,(\mathbf{v}(t) \bullet \mathbf{v}(t+1)]$. The MSD of a cell at time *t* is calculated by $MSD(\tau) = < r(t+\tau) - r(t) >$, as a function of lag time τ. MSD values are calculated across the entire trajectory for lag times *τ* ranging from 1 to 800 frames (0.017 to 13.3 s). Cells exhibiting circular motility patterns are expected to show plateaus at long-time MSDs. Plots of time-averaged MSD for each cell are shown as grey lines in Figure S3B; ensemble-averages are shown for each species in red. For interspecies comparisons (Figure 1C), ensemble-averaged MSDs for each species were normalised by dividing by the MSD value at τ = *1.*

Fluorescence assays

In all cases, zoospores were collected from the suspension medium by centrifugation at 1000 x g for 5 min followed by removal of the supernatant in order to concentrate the cells. In all cases the cell pellet was fixed in 0.5 ml of 4% *w/v* paraformaldehyde in 1X PBS and transferred into a 15 ml Falcon tube for 15 min at room temperature. Cells were concentrated by centrifugation and resuspended in PBS for the first washing step. The cell pellet was then resuspended and permeabilized in 0.5 ml of PBS containing 0.1% *v/v* Triton X-100 in PBS. A second washing step in 0.5 ml of PBS was performed and then the cells were blocked with 0.5 ml of 1% *w/v* BSA in PBS and incubated for 45 min at room temperature, followed by the addition of the primary antibody α-tubulin DM1A (Sigma-Aldrich, Cat# T6199, RRID: AB_477583) at a concentration of 1:500 v/v in 1% *w/v* BSA in PBS for 180 min at room temperature. After a third washing step of the primary antibody with 1X PBS, the secondary antibody Alexa Fluor 647 Goat anti-mouse IgG1 antibody was added (Thermo Fisher Scientific, Cat#A-21240, RRID: AB_2535809) to the PBS-resuspended fixed zoospore solution for 60 min at room temperature. Alexa Fluor 488 Phalloidin (Invitrogen, Cat# A12379, RRID: AB_2759222) and Nile Red (Thermo Fisher Scientific, Cat# N1142) were also added at a 1:500 v/v concentration for 60 min at room temperature. After two washing steps with 1X PBS, the final cell pellets were resuspended in 100 µl of 20% v/v Citifluor AF2 Antifadent Mountant Solution and 7 µl was placed on a slide and covered with a coverslip, which was then sealed with transparent nail polish on the edges to avoid evaporation. Cells were imaged

on a Zeiss LSM-780 inverted high-resolution laser scanning confocal microscope with a Ph3 ×100 oil objective. Exposures were kept constant during experiments, and images collected using ZEISS ZEN Software (ZEN Digital Imaging for Light Microscopy), and analysed/formatted with Fiji [57].

References

1. James, T.Y., Porter, T.M., and Martin, W.W. (2014). Blastocladiomycota. Syst. Evol., 177–207.
2. Powell, M.J. (2017). Chytridiomycota. In Handbook of the Protists: Second Edition, pp. 1523–1558.
3. Sparrow, F.K. (1960). Aquatic Phycomycetes. Univ. Michigan Press *132*.
4. Naranjo-Ortiz, M.A., and Gabaldón, T. (2019). Fungal evolution: major ecological adaptations and evolutionary transitions. Biol. Rev. *94*, 1443–1476.
5. Kagami, M., de Bruin, A., Ibelings, B.W., and Van Donk, E. (2007). Parasitic chytrids: their effects on phytoplankton communities and food-web dynamics. Hydrobiologia *578*, 113–129.
6. Gleason, F.H., Kagami, M., Lefevre, E., and Sime-Ngando, T. (2008). The ecology of chytrids in aquatic ecosystems: roles in food web dynamics. Fungal Biol. Rev. *22*, 17–25.
7. Kagami, M., Miki, T., and Takimoto, G. (2014). Mycoloop: Chytrids in aquatic food webs. Front. Microbiol. *5*, 166.
8. Cheng, T.L., Rovito, S.M., Wake, D.B., and Vredenburg, V.T. (2011). Coincident mass extirpation of neotropical amphibians with the emergence of the infectious fungal pathogen *Batrachochytrium dendrobatidis*. Proc. Natl. Acad. Sci. *108*, 9502–9507.
9. Gleason, F.H., and Lilje, O. (2009). Structure and function of fungal zoospores: ecological implications. Fungal Ecol. *2*, 53–59.
10. Trinci, A.P.J., Davies, D.R., Gull, K., Lawrence, M.I., Bonde Nielsen, B., Rickers, A., and Theodorou, M.K. (1994). Anaerobic fungi in herbivorous animals. Mycol. Res. *98*, 129–152.
11. Ustinova, I., Krienitz, L., and Huss, V.A.R. (2000). Hyaloraphidium curvatum is not a green alga but a lower fungus; Amoebidium parasiticum is not a fungus, but a member of the DRIPs. Protist *151*, 253–262.
12. Barr, D.J.S. (2001). Chytridiomycota. In The Mycota, D. J. McLaughlin, E. G. McLaughlin, and P. A. Lemke, eds. (Springer Berlin Heidelberg), pp. 93–112.
13. Galindo, L.J., López-García, P., Torruella, G., Karpov, S., and Moreira, D. (2021). Phylogenomics of a new fungal phylum reveals multiple waves of reductive evolution across Holomycota. Nat. Commun. *12*, 4973.

14. Strittmatter, M., Guerra, T., Silva, J., and Gachon, C.M.M. (2016). A new flagellated dispersion stage in Paraphysoderma sedebokerense, a pathogen of Haematococcus pluvialis. J. Appl. Phycol. *28*, 1553–1558.
15. Prostak, S.M., Robinson, K.A., Titus, M.A., and Fritz-Laylin, L.K. (2021). The actin networks of chytrid fungi reveal evolutionary loss of cytoskeletal complexity in the fungal kingdom. Curr. Biol. *31*, 1192-1205.e6.
16. Moss, A.S., Reddy, N.S., Dortaj, I.M., and San Francisco, M.J. (2008). Chemotaxis of the amphibian pathogen Batrachochytrium dendrobatidis and its response to a variety of attractants. Mycologia *100*, 1–5.
17. Avelar, G.M., Schumacher, R.I., Zaini, P.A., Leonard, G., Richards, T.A., and Gomes, S.L. (2014). A Rhodopsin-Guanylyl cyclase gene fusion functions in visual perception in a fungus. Curr. Biol. *24*, 1234–1240.
18. Swafford, A.J.M., and Oakley, T.H. (2018). Multimodal sensorimotor system in unicellular zoospores of a fungus. J. Exp. Biol. *221*.
19. Wang, Y., Verbrugghe, E., Meuris, L., Chiers, K., Kelly, M., Strubbe, D., Callewaert, N., Pasmans, F., and Martel, A. (2021). Epidermal galactose spurs chytrid virulence and predicts amphibian colonization. Nat. Commun. *12*, 5788.
20. Bentley, S.A., Laeverenz-Schlogelhofer, H., Anagnostidis, V., Cammann, J., Mazza, M.G., Gielen, F., and Wan, K.Y. (2022). Phenotyping single-cell motility in microfluidic confinement. Elife *11*, e76519.
21. Bondoc-Naumovitz, K.G., Laeverenz-Schlogelhofer, H., Poon, R.N., Boggon, A.K., Bentley, S.A., Cortese, D., and Wan, K.Y. (2023). Methods and Measures for Investigating Microscale Motility. Integr. Comp. Biol. *63*, 1485–1508.
22. Canter, H.M., and Jaworski, G.H.M. (1980). Some General Observations on Zoospores of the Chytrid Rhizophydium planktonicum Canter Emend. New Phytol. *84*, 515–531.
23. Sparrow, F.K., and Johns, R.M. (1970). Observations on chytridiaceous parasites of phanerogams. Arch. Mikrobiol. *70*, 72–81.
24. Fuller, M.S., and Olson, L.W. (1971). The zoospore of Allomyces. Microbiology *66*, 171–183.
25. Reichle, R.E., and Fuller, M.S. (1967). The fine structure of Blastocladiella emersonii zoospores. Am. J. Bot. *54*, 81–92.
26. Letcher, P.M., Powell, M.J., Churchill, P.F., and Chambers, J.G. (2006). Ultrastructural and molecular phylogenetic delineation of a new order, the Rhizophydiales (Chytridiomycota). Mycol. Res. *110*, 898–915.
27. Simmons, D.R., James, T.Y., Meyer, A.F., and Longcore, J.E. (2009). Lobulomycetales, a new order in the Chytridiomycota. Mycol. Res. *113*, 450–460.

28. Simmons, D.R. (2011). Phylogeny of Powellomycetaceae fam. nov. and description of Geranomyces variabilis gen. et comb. nov. Mycologia *103*, 1411–1420.
29. Longcore, J.E., Letcher, P.M., and James, T.Y. (2012). Homolaphlyctis polyrhiza gen. et sp. nov., a species in the Rhizophydiales (Chytridiomycetes) with multiple rhizoidal axes. Mycotaxon *118*, 433–440.
30. Letcher, P.M., Powell, M.J., Barr, D.J.S., Churchill, P.F., Wakefield, W.S., and Picard, K.T. (2008). Rhizophlyctidales--a new order in Chytridiomycota. Mycol. Res. *112*, 1031–1048.
31. Barr, D.J.S. (1984). Cytological variation in zoospores of Spizellomyces (Chytridiomycetes). Can. J. Bot. *62*, 1202–1208.
32. Barr, D.J.S. (1980). An outline for the reclassification of the Chytridiales, and for a new order, the Spizellomycetales. Can. J. Bot. *58*, 2380–2394.
33. Venard, C.M., Vasudevan, K.K., and Stearns, T. (2020). Cilium axoneme internalization and degradation in chytrid fungi. Cytoskeleton *77*, 365–378.
34. Simmons, D.R., Bonds, A.E., Castillo, B.T., Clemons, R.A., Glasco, A.D., Myers, J.M., Thapa, N., Letcher, P.M., Powell, M.J., Longcore, J.E., et al. (2020). The Collection of Zoosporic Eufungi at the University of Michigan (CZEUM): introducing a new repository of barcoded Chytridiomyceta and Blastocladiomycota cultures. IMA Fungus *11*, 20.
35. Powell, M.J. (1978). Phylogenetic implications of the microbody-lipid globule complex in zoosporic fungi. BioSystems *10*, 167–180.
36. Dawson, S.C., Sagolla, M.S., Mancuso, J.J., Woessner, D.J., House, S.A., Fritz-Laylin, L., and Cande, W.Z. (2007). Kinesin-13 regulates flagellar, interphase, and mitotic microtubule dynamics in Giardia intestinalis. Eukaryot. Cell *6*, 2354–2364.
37. Toba, S., Fox, L.A., Sakakibara, H., Porter, M.E., Oiwa, K., and Sale, W.S. (2011). Distinct roles of 1alpha and 1beta heavy chains of the inner arm dynein I1 of Chlamydomonas flagella. Mol. Biol. Cell *22*, 342–353.
38. Kapoor, P., Sachdeva, M., and Madhubala, R. (1999). Effect of the microtubule stabilising agent taxol on leishmanial protozoan parasites in vitro. FEMS Microbiol. Lett. *176*, 429–435.
39. Herth, W. (1983). Taxol effects cytoskeletal microtubules, flagella and spindle structure of the chrysoflagellate alga Poterioochromonas. Protoplasma *115*, 228–239.
40. Wang, L., Piao, T., Cao, M., Qin, T., Huang, L., Deng, H., Mao, T., and Pan, J. (2013). Flagellar regeneration requires cytoplasmic microtubule depolymerization and kinesin-13. J. Cell Sci. *126*, 1531–1540.
41. Laundon, D., Chrismas, N., Bird, K., Thomas, S., Mock, T., and Cunliffe, M. (2022). A cellular and molecular atlas reveals the basis of chytrid development. Elife *11*,

622 e73933.
623 42. Richards, T.A., and Gomes, S.L. (2015). How to build a microbial eye. Nature *523*,
624 166–167.
625 43. Robinson, K.A., Prostak, S.M., Campbell Grant, E.H., and Fritz-Laylin, L.K. (2022).
626 Amphibian mucus triggers a developmental transition in the frog-killing chytrid fungus.
627 Curr. Biol. *32*, 2765-2771.e4.
628 44. Cantino, E.C., and Truesdell, L.C. (1970). Organization and fine structure of the side
629 body and its lipid sac in the zoospore of Blastocladiella emersonii. Mycologia *62*, 548–
630 567.
631 45. Galindo, L.J., Milner, D.S., Gomes, S.L., and Richards, T.A. (2022). A light-sensing
632 system in the common ancestor of the fungi. Curr. Biol. *32*, 3146-3153.e3.
633 46. KAZAMA, F.Y. (1972). Ultrastructure and Phototaxis of the Zoospores of
634 Phlyctochytrium sp., an Estuarine Chytrid. Microbiology *71*, 555–566.
635 47. Robertson, J.A. (1972). Phototaxis in a new Allomyces. Arch. Mikrobiol.
636 48. Saranak, J., and Foster, K.W. (1997). Rhodopsin guides fungal phototaxis. Nature
637 *387*, 465–466.
638 49. Avelar, G.M., Glaser, T., Leonard, G., Richards, T.A., Ulrich, H., and Gomes, S.L.
639 (2015). A cyclic GMP-dependent K+ channel in the blastocladiomycete fungus
640 Blastocladiella emersonii. Eukaryot. Cell *14*, 958–963.
641 50. Gao, S., Nagpal, J., Schneider, M.W., Kozjak-Pavlovic, V., Nagel, G., and Gottschalk,
642 A. (2015). Optogenetic manipulation of cGMP in cells and animals by the tightly light-
643 regulated guanylyl-cyclase opsin CyclOp. Nat. Commun. *6*, 1–12.
644 51. Broser, M., Spreen, A., Konold, P.E., Peter, E., Adam, S., Borin, V., Schapiro, I.,
645 Seifert, R., Kennis, J.T.M., Bernal Sierra, Y.A., et al. (2020). NeoR, a near-infrared
646 absorbing rhodopsin. Nat. Commun. *11*, 5682.
647 52. Broser, M., Busse, W., Spreen, A., Reh, M., Sierra, Y.A.B., Hwang, S., Utesch, T.,
648 Sun, H., and Hegemann, P. (2023). Diversity of rhodopsin cyclases in zoospore-
649 forming fungi. Proc. Natl. Acad. Sci. *120*, e2310600120.
650 53. Amses, K.R., Simmons, D.R., Longcore, J.E., Mondo, S.J., Seto, K., Jerônimo, G.H.,
651 Bonds, A.E., Quandt, C.A., Davis, W.J., Chang, Y., et al. (2022). Diploid-dominant life
652 cycles characterize the early evolution of Fungi. Proc. Natl. Acad. Sci. U. S. A. *119*,
653 e2116841119.
654 54. Powell, M.J. (2014). Hypothesized evolutionary trends in zoospore ultrastructural
655 characters in Chytridiales (Chytridiomycota). *106*, 379–396.
656 55. Reid, B., Morris, B.M., and Gow, N.A.R. (1995). Calcium-Dependent, Genus-Specific,
657 Autoaggregation of Zoospores of Phytopathogenic Fungi. Exp. Mycol. *19*, 202–213.
658 56. Byrt, P.N., Irving, H.R., and Grant, B.R. (1982). The Effect of Cations on Zoospores of

the Fungus Phytophthora cinnamomi. Microbiology *128*, 1189–1198.

57. Schindelin, J., Arganda-Carreras, I., Frise, E., Kaynig, V., Longair, M., Pietzsch, T., Preibisch, S., Rueden, C., Saalfeld, S., Schmid, B., et al. (2012). Fiji: an open-source platform for biological-image analysis. Nat. Methods *9*, 676–682.

58. Tinevez, J.-Y., Perry, N., Schindelin, J., Hoopes, G.M., Reynolds, G.D., Laplantine, E., Bednarek, S.Y., Shorte, S.L., and Eliceiri, K.W. (2017). TrackMate: An open and extensible platform for single-particle tracking. Methods *115*, 80–90.

59. Anderson, D.P., Whitney, D.S., Hanson-Smith, V., Woznica, A., Campodonico-Burnett, W., Volkman, B.F., King, N., Thornton, J.W., and Prehoda, K.E. (2016). Evolution of an ancient protein function involved in organized multicellularity in animals. Elife *5*, e10147.

Graphical Abstract

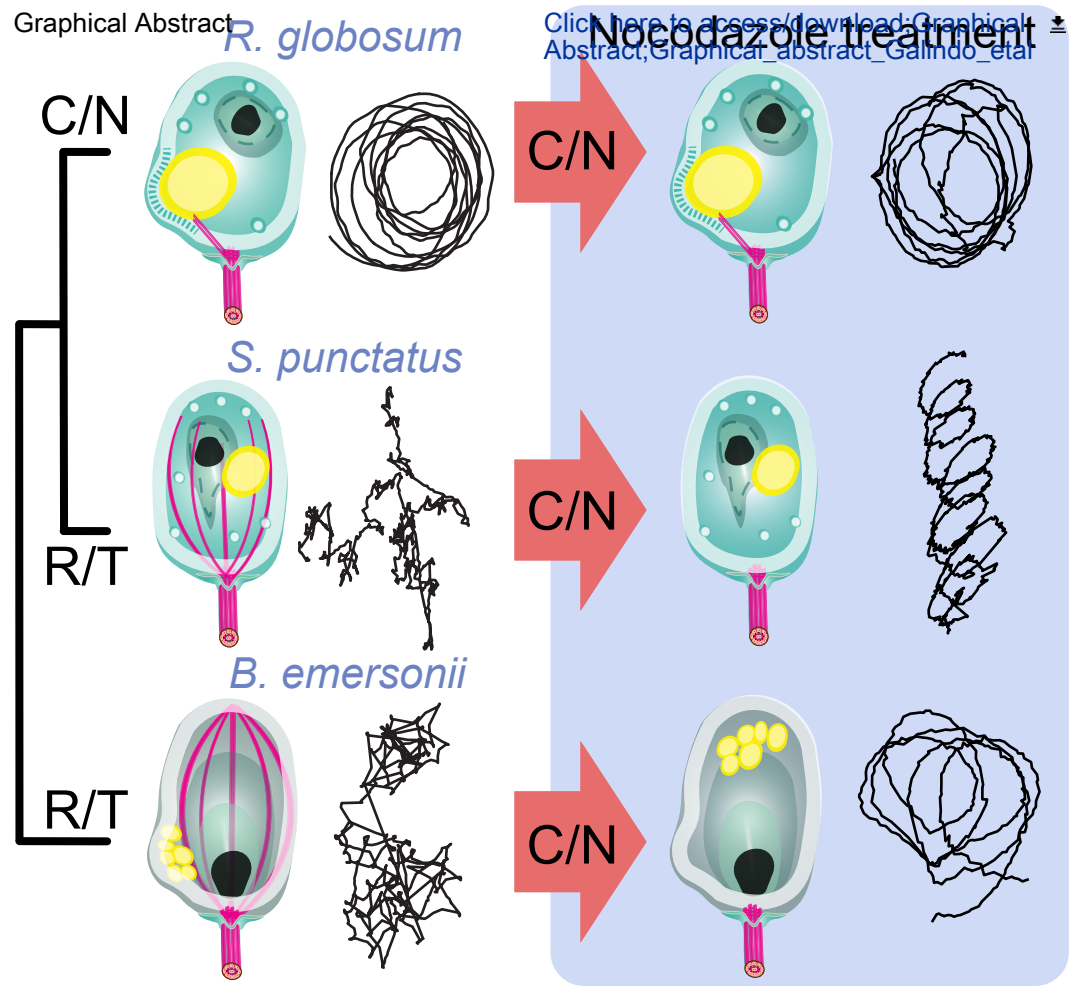

Swimming pattern: Circular (**C**) vs Random walk (**R**)
Cytoplasmic tubulin component: Prominent (**T**) or not (**N**)

Figure 1

A compiled tracks show cytology-specific behaviors

all scale bars denote 50 μm

random walk patterns in Blastocladiomycota species

Be (n=37) *Ar* (n=45) *Am* (n=68) *Cat* (n=90)

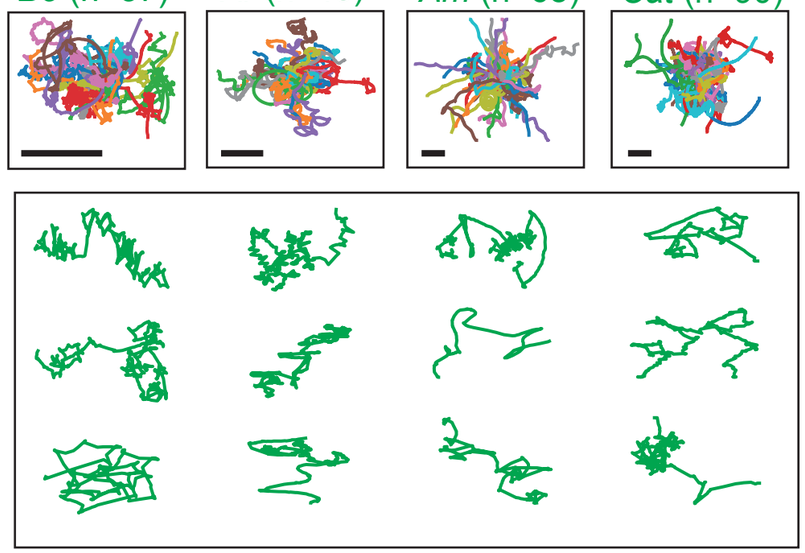

random walk patterns in Chytridiomycota species with prominent cytoplasmic tubulin structures

Gv (n=101) *Rr* (n=49) *Cv* (n=96) *Sp* (n=77)

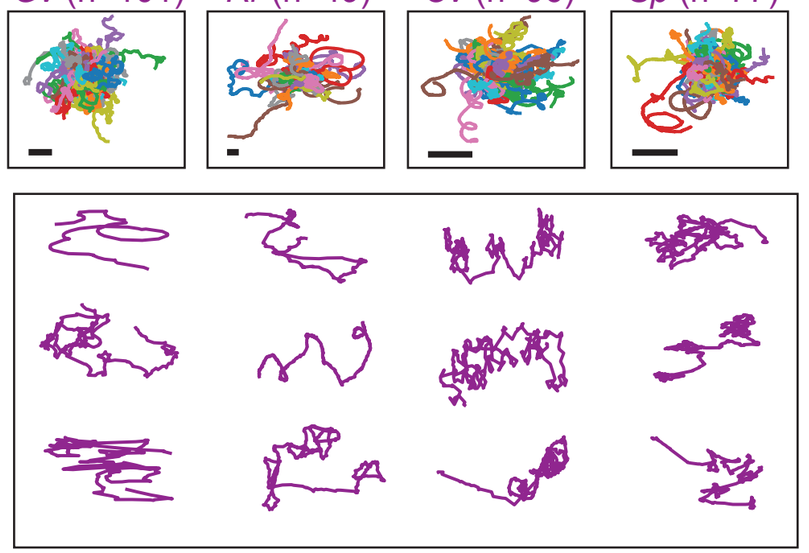

circular swimming in Chytridiomycota species without prominent cytoplasmic tubulin structures

Rg (n=66) *Ch* (n=21) *Sm* (n=21) *Hp* (n=23)

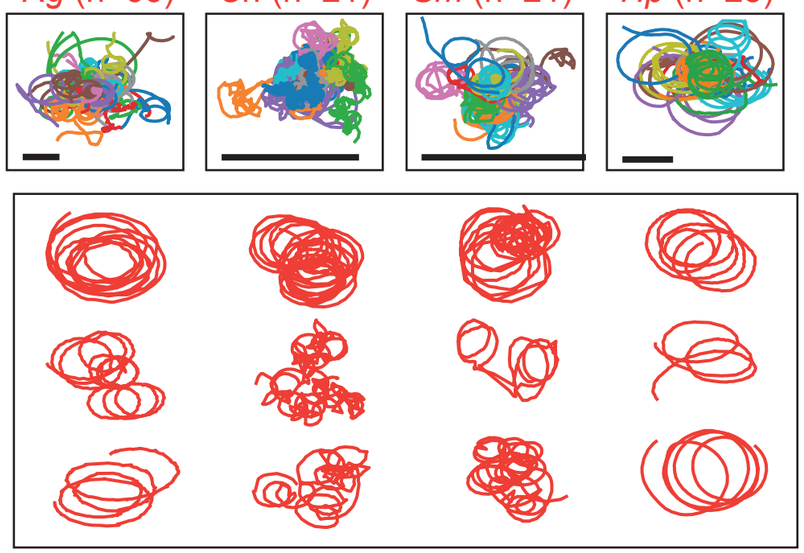

shorter and longer timescale motility dynamics vary across groups

B reorientation angle distribution

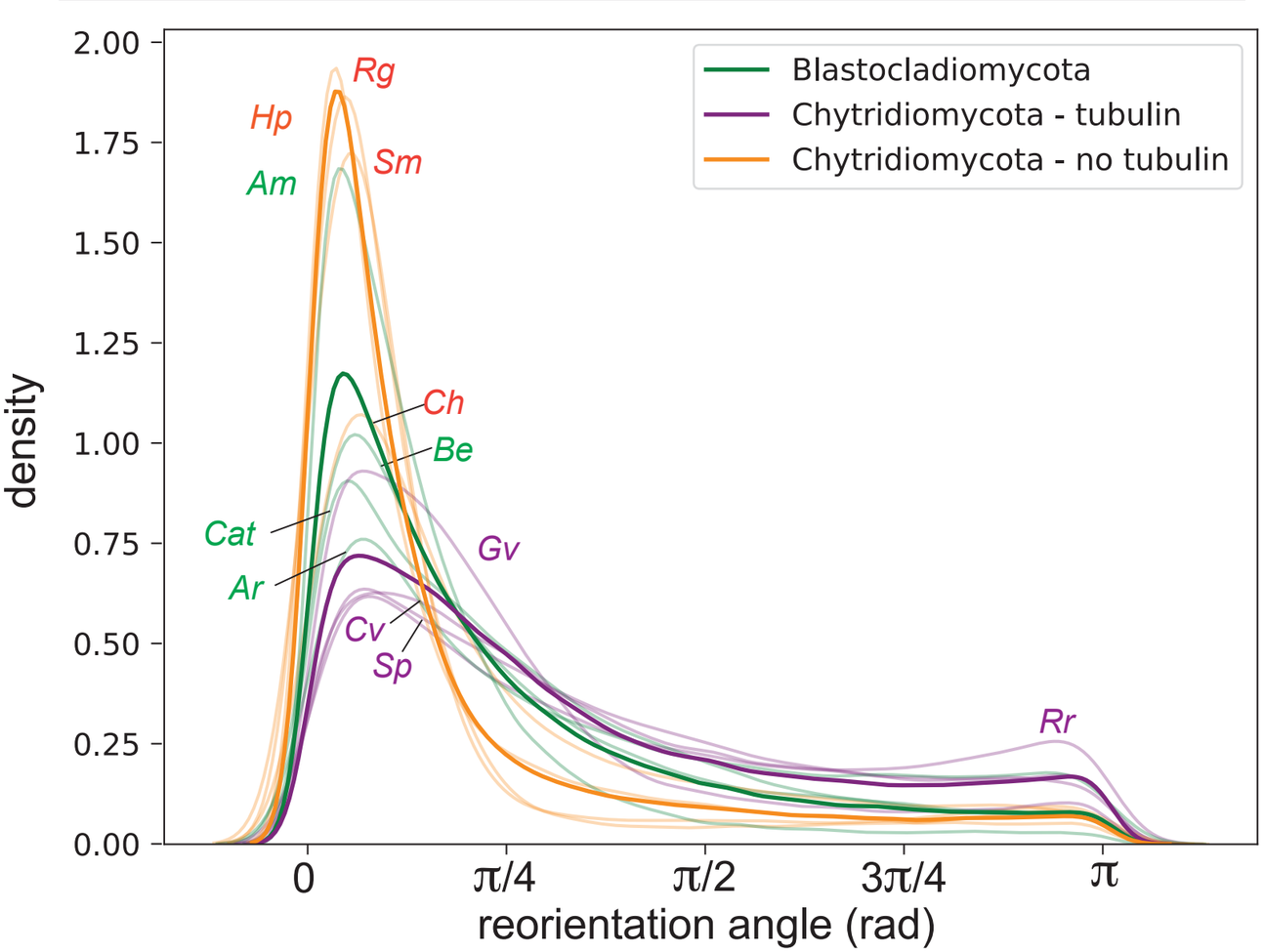

C mean squared displacement

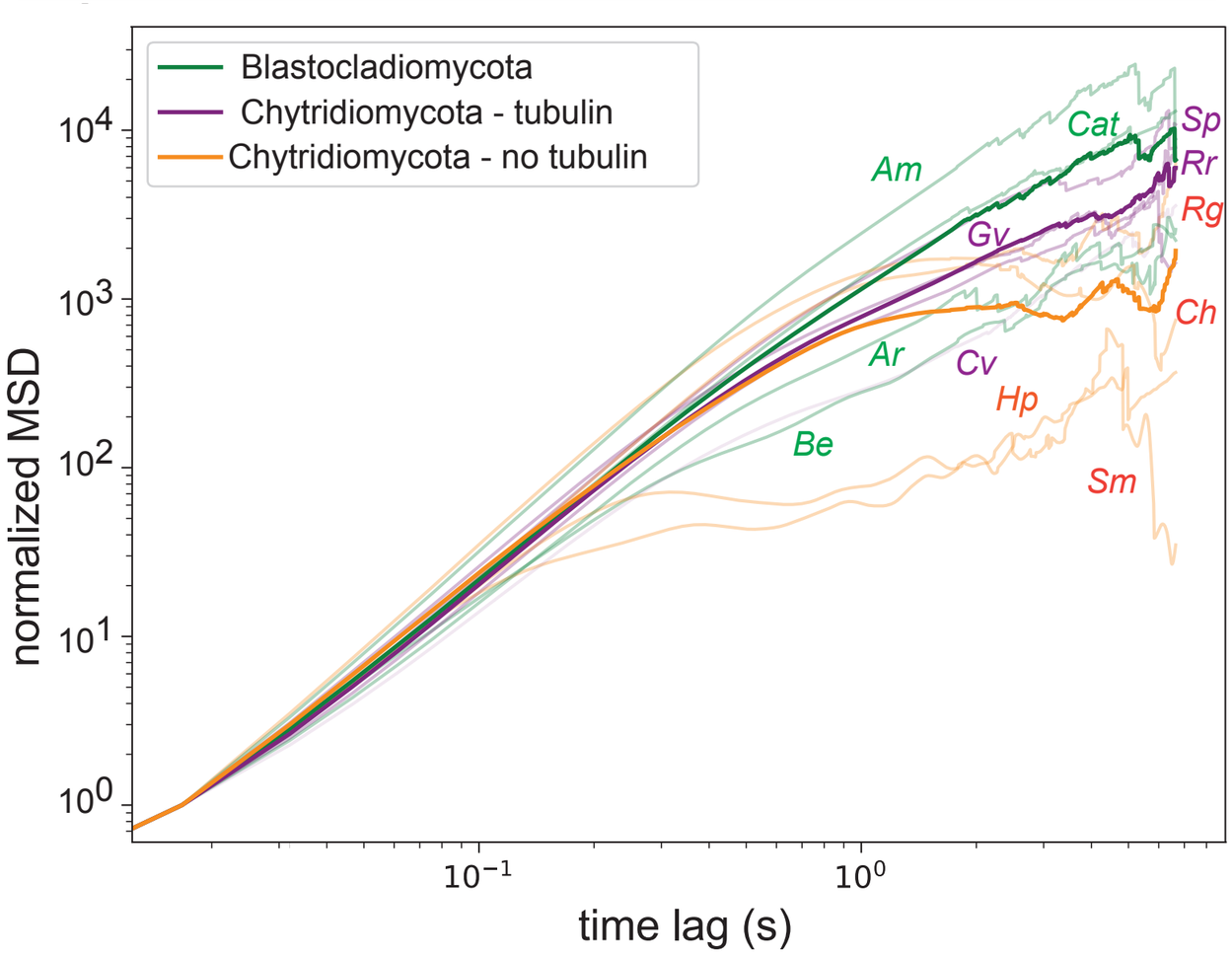

Figure 3

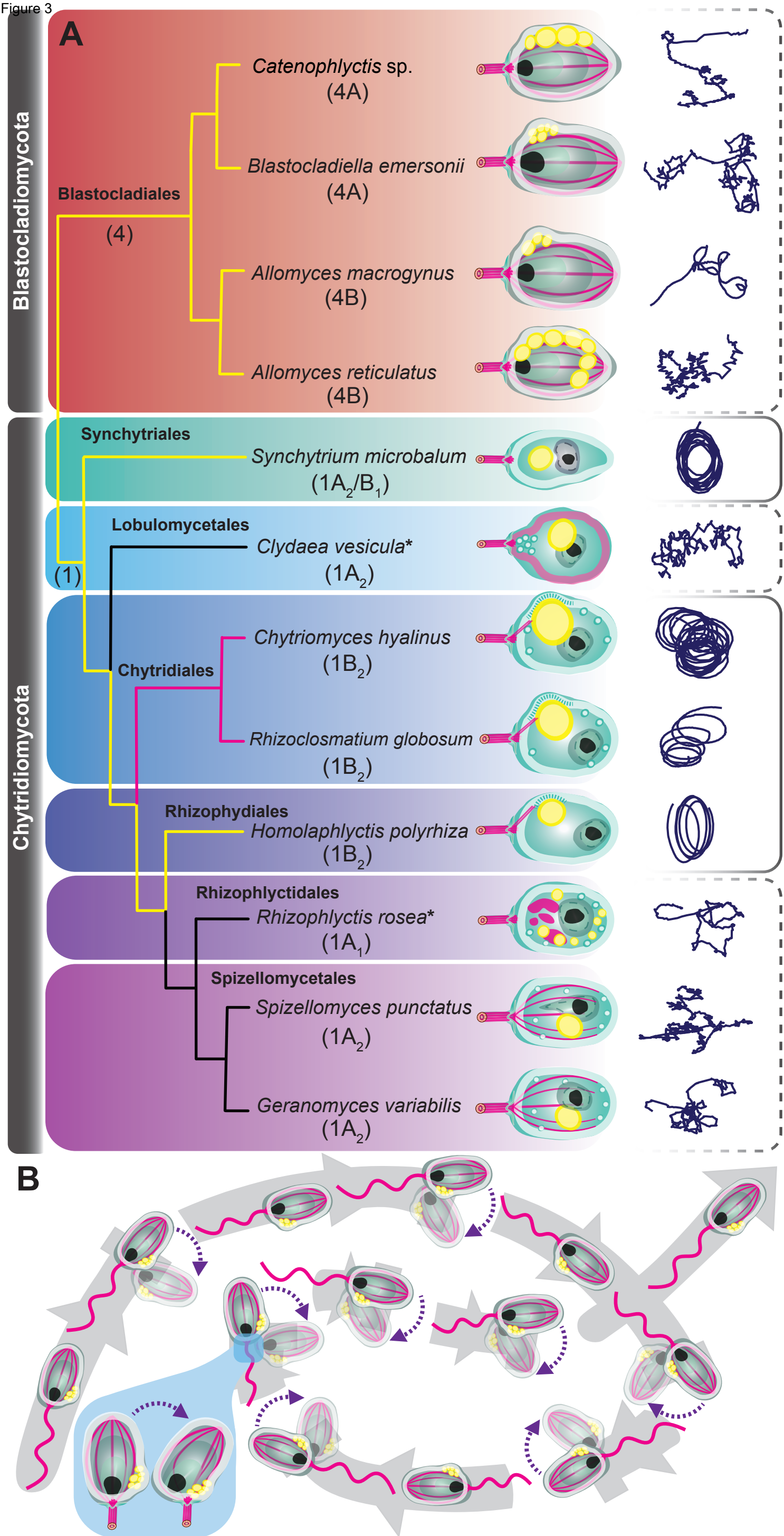
A
Blastocladiomycota
Blastocladiales
(4)
Catenophlyctis sp.
(4A)
Blastocladiella emersonii
(4A)
Allomyces macrogynus
(4B)
Allomyces reticulatus
(4B)
Chytridiomycota
Synchytriales
Synchytrium microbalum
(1A2/B1)
Lobulomycetales
(1)
Clydaea vesicula*
(1A2)
Chytridiales
Chytriomyces hyalinus
(1B2)
Rhizoclosmatium globosum
(1B2)
Rhizophydiales
Homolaphlyctis polyrhiza
(1B2)
Rhizophlyctidales
Rhizophlyctis rosea*
(1A1)
Spizellomycetales
Spizellomyces punctatus
(1A2)
Geranomyces variabilis
(1A2)
B

Figure 4

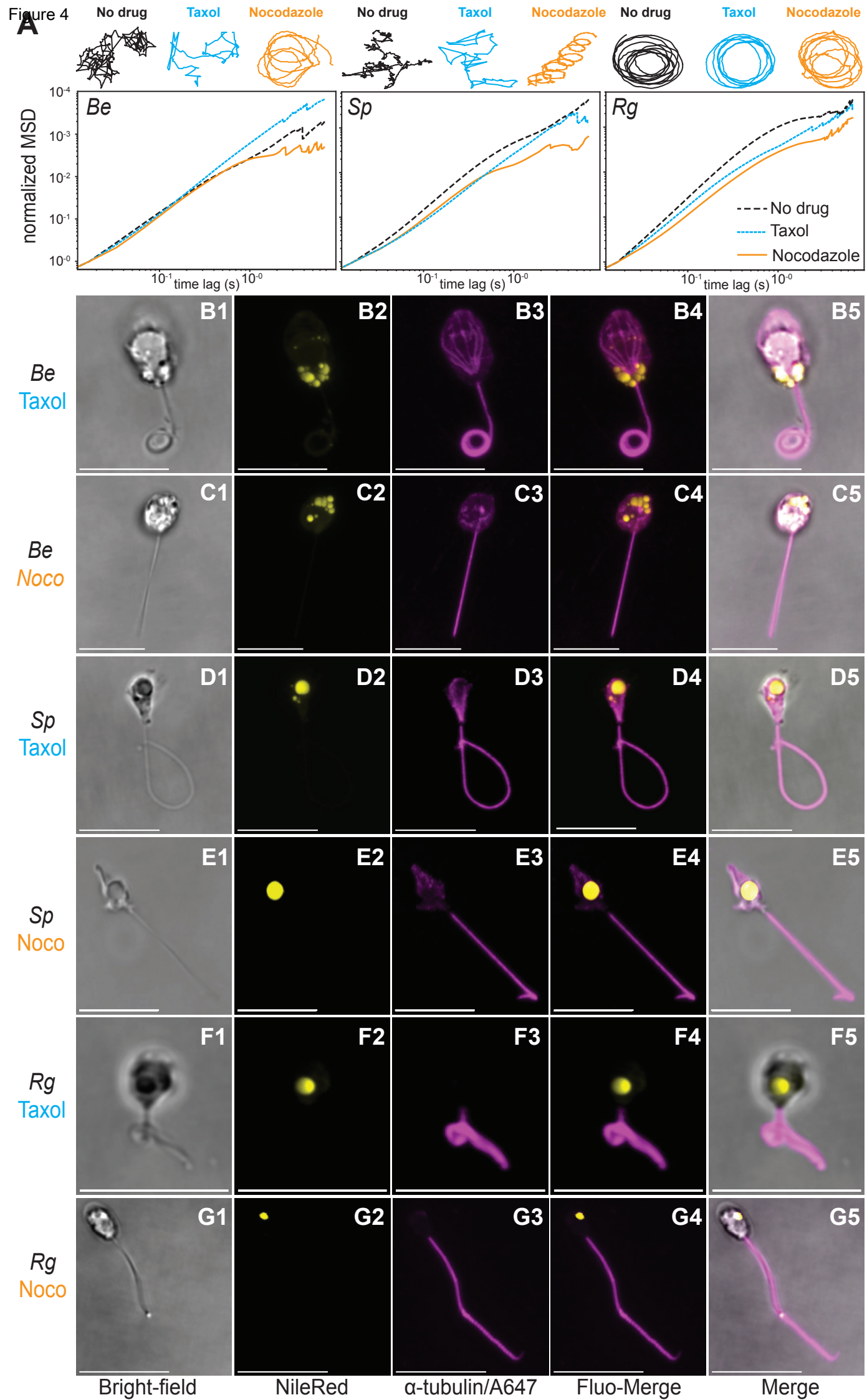
A
No drug
Taxol
Nocodazole
No drug
Taxol
Nocodazole
No drug
Taxol
Nocodazole
normalized MSD
Be
Sp
Rg
time lag (s)
No drug
Taxol
Nocodazole
Be Taxol
Be Noco
Sp Taxol
Sp Noco
Rg Taxol
Rg Noco
B1
B2
B3
B4
B5
C1
C2
C3
C4
C5
D1
D2
D3
D4
D5
E1
E2
E3
E4
E5
F1
F2
F3
F4
F5
G1
G2
G3
G4
G5
Bright-field
NileRed
α-tubulin/A647
Fluo-Merge
Merge

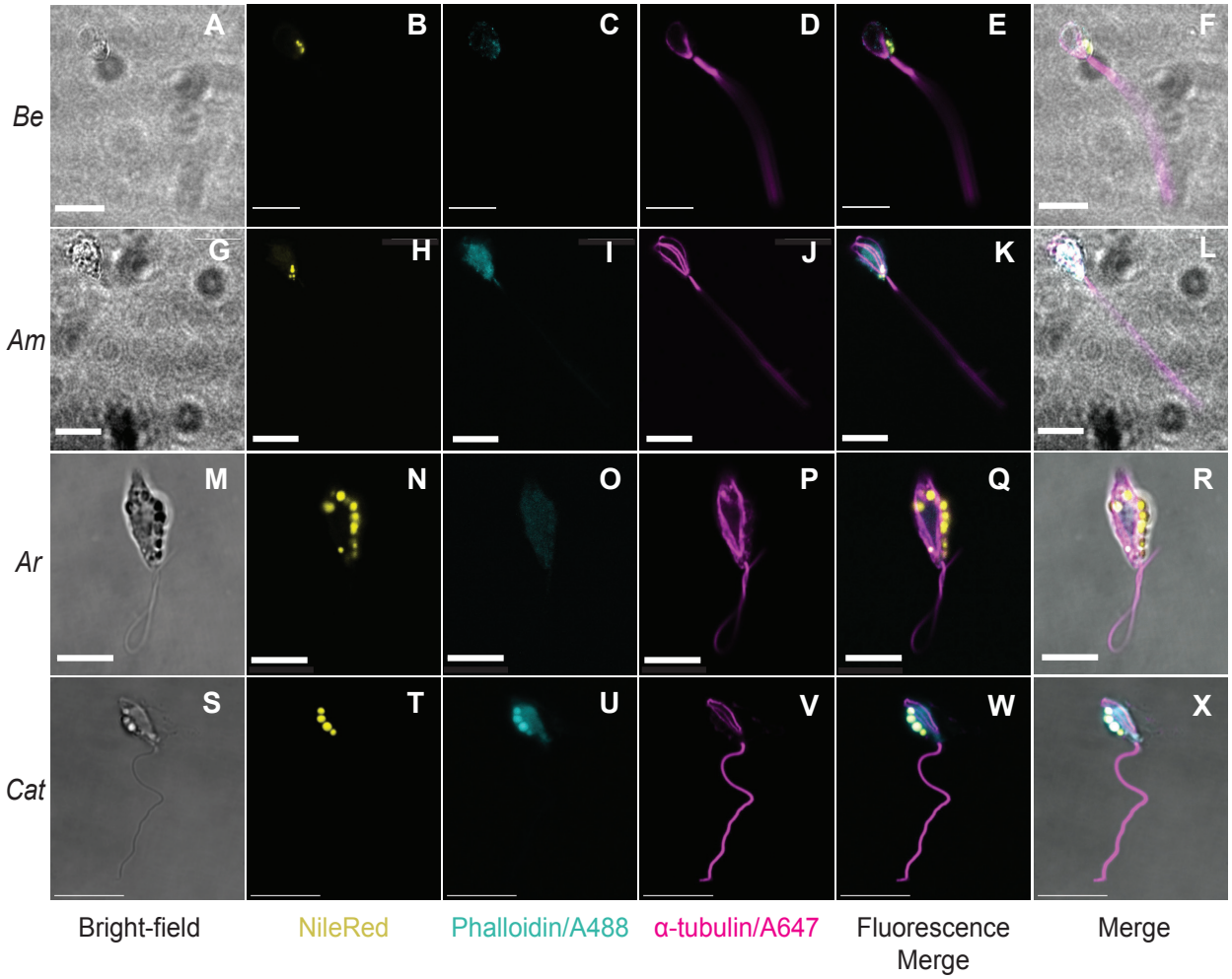

Figure S1. Imaging of ultrastructure in Blastocladiomycota zoospores, related to Figure 2. First columns show brightfield phase contrast confocal microscopy images (A, G, M, S). Second columns show fluorescent confocal microscopy micrograph of the zoospore stained with with NileRed to stain lipid droplets (B, H, N, T; yellow). Third column shows zoospores stained with Alexa Fluor 488 Phalloidin to stain actin (C, I, O, U; cyan). Fourth column shows α-tubulin DM1A + Alexa Fluor 647 staining for α-tubulin (D, J, P, V, magenta). The fifth column shows the merge of all fluorescent channels (E, D, J, P, V). The sixth column shows the merged images of brightfield and fluorescent channels (F, L, R, X). Scale bars: A1-O1 = 10 μm; P1-D2 = 5 μm. Scale bars in small α-tubulin panels: B1, E1, H1 = 10 μm; K1, Q1, W1, Z1 and C2 = 5 μm. Labels: *Catenophlyctis* sp.: *Cat, Blastocladiella emersonii*: *Be, Allomyces macrogynus*: *Am, Allomyces reticulatus: Ar*.

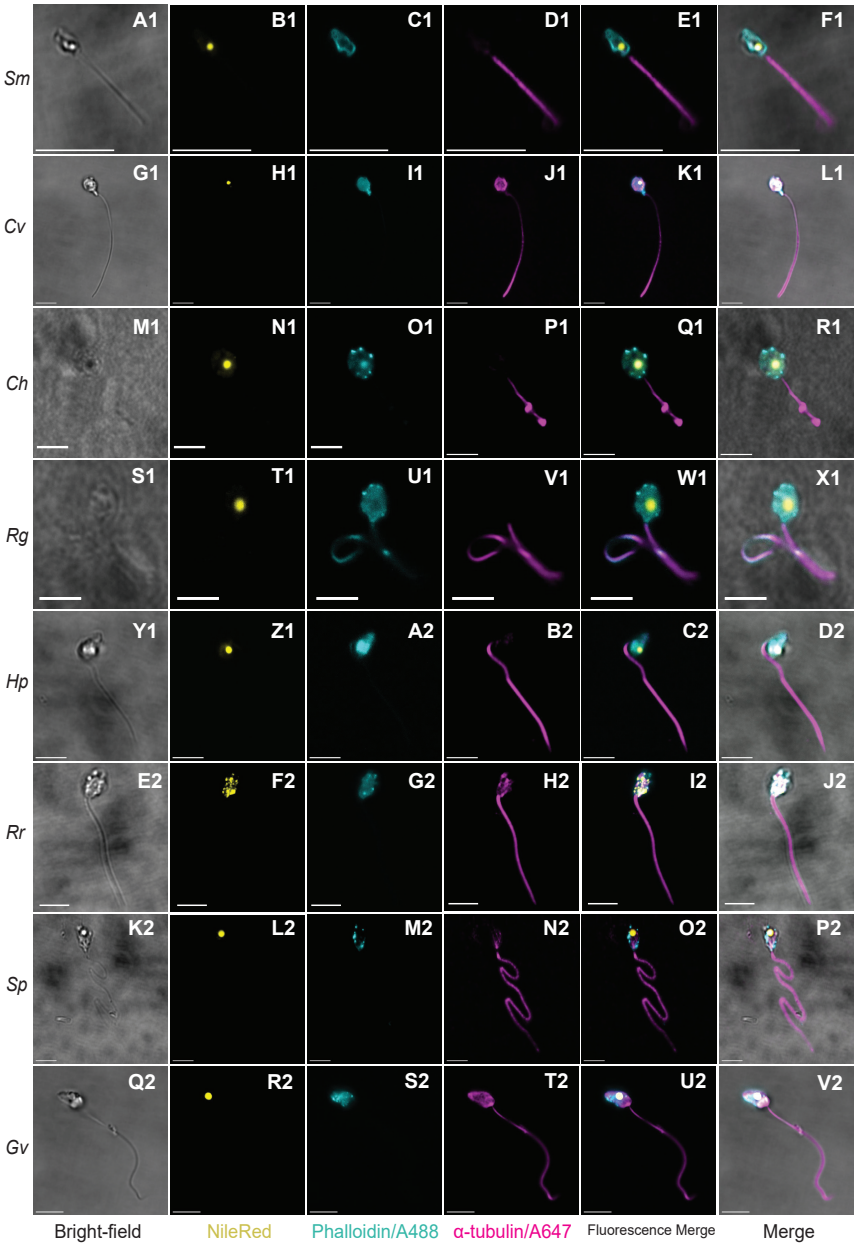

Figure S2. Imaging of ultrastructure in Chytridiomycota zoospores, related to Figure 2. First columns show brightfield phase contrast confocal microscopy images (A1, G1, M1, S1, Y1, E2, K2, Q2). Second columns show fluo- rescent confocal microscopy micrograph of the zoospore stained with with NileRed to stain lipid droplets (B1, H1, N1, T1, Z1, F2, L2, R2; yellow). Third column shows zoospores stained with Alexa Fluor 488 Phalloidin to stain actin (C1, I1, O1, U1, A2, G2, M2, S2; cyan). Fourth column shows α-tubulin DM1A + Alexa Fluor 647 staining for α-tubulin (D1, J1, P1, V1, B2, H2, N2, T2; magenta). The fifth column shows the merge of all fluorescent channels (E1, K1, Q1, W1, C2, I2, O2, U2). The sixth column shows the merged images of brightfield and fluorescent channels (F1, L1, R1, X1, D2, J2, P2, V2). Scale bars: A1-O1 = 10 µm; P1-D2 = 5 µm. Scale bars in small α-tubulin panels: B1, E1, H1 = 10 µm; K1, Q1, W1, Z1 and C2 = 5 µm. *Synchytrium microbalum: Sm, Clydaea vesicula: Cv, Chytriomyces hyalinus: Ch, Rhizoclosmatium globosum: Rg, Homolaphlyctis polyrhiza: Hp, Rhizophlyctis rosea: Rr, Geranomyces variabilis: Gv, and Spizellomyces punctatus: Sp.*

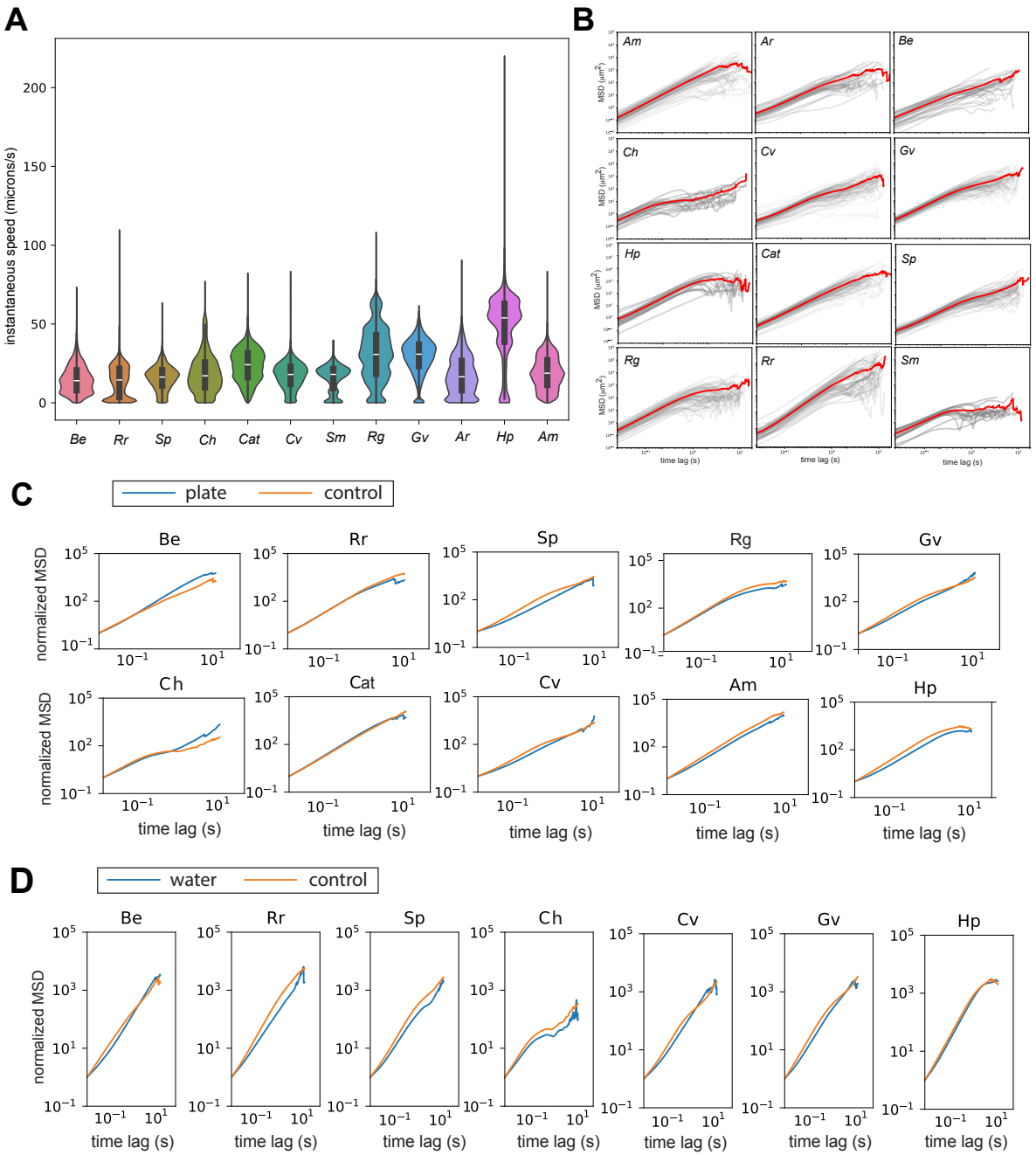

Figure S3. Motility metrics, related to Figure 1. (A) Instantaneous speeds (in units of microns per second) over all trials for each fungal zoospore species. **(B)** Time averaged MSD values (grey lines) and ensemble averaged MSD values (red lines) for each fungal zoospore species. Time- and ensemble-averaged MSDs comparing the motility dynamics of various zoospore species in **(C)** an unconfined environment (86-well plate) and **(D)** water as opposed to a control condition in between two coverslips in media as denoted in the main text.

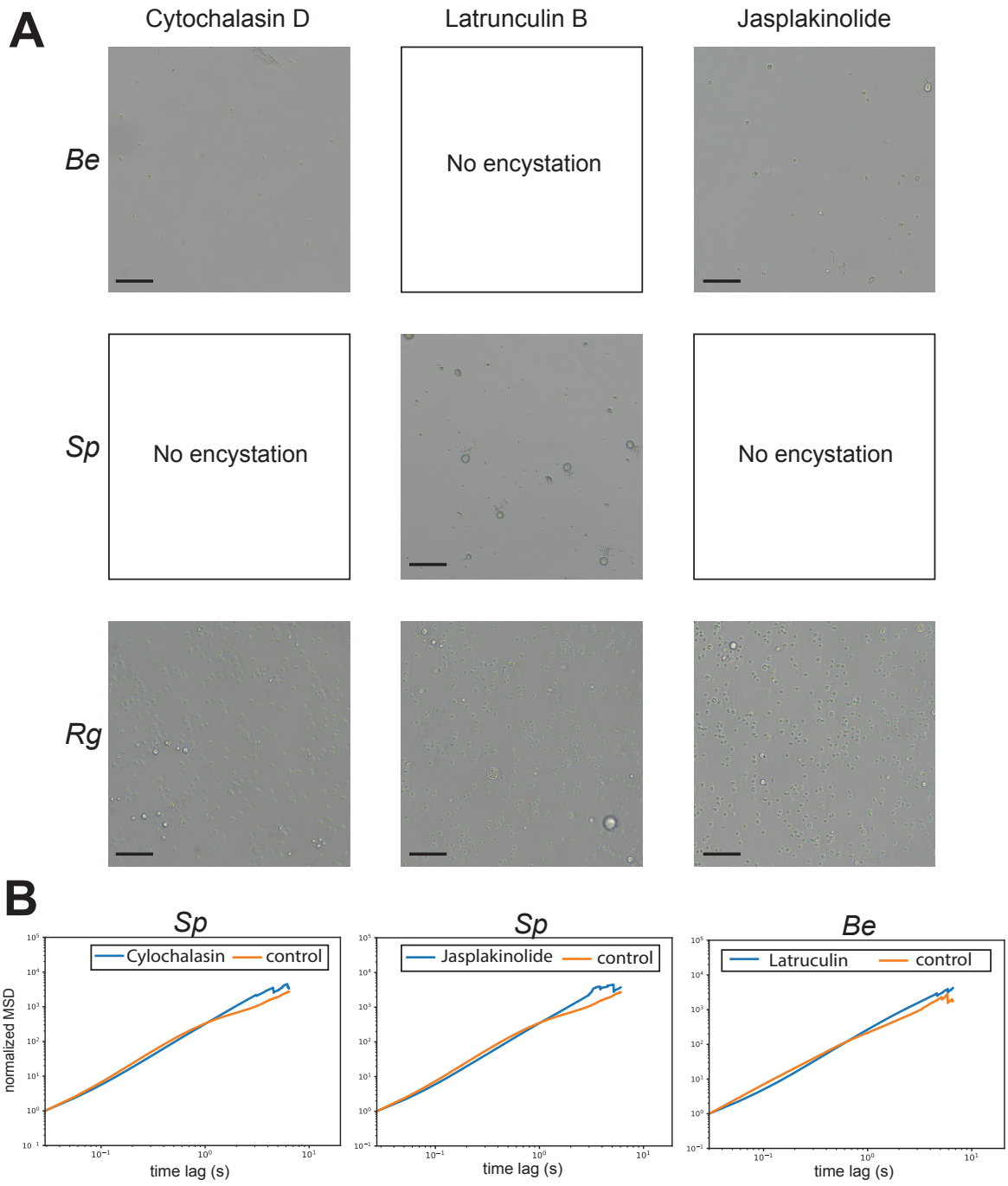

Figure S4. **Effects of drugs, related to Figure 4.** (A) Encystation in zoospores from three fungal species after exposure to actin depolymerizing drugs. Zoospore solution of these three species was alternatively exposed for 10 min at RT to 1 μM Latrunculin B (to sequester actin monomers), 100 μM Cytochalasin D (to cap actin filaments), 10 μM Jasplakinolide (to stabilize actin filaments) solutions resuspended on DMSO before being recorded. Scale bars = 50 μm. (B) Time- and ensemble-averaged MSDs comparing motility patterns after exposure to actin depolymerizing drugs. *Blastocladiella emersonii: Be, Spizellomyces punctatus: Sp, Rhizoclosmatium globosum: Rg*.